

- Access to high resolution figures
- Links to articles and content related to this article
- Copyright permission to reproduce figures and/or text from this article

[View the Full Text HTML](#)



Effect of Anchoring Groups on Single-Molecule Conductance: Comparative Study of Thiol-, Amine-, and Carboxylic-Acid-Terminated Molecules

Fang Chen, Xiulan Li, Joshua Hihath, Zhifeng Huang, and Nongjian Tao*

Department of Electrical Engineering & Center for Solid State Electronics Research, Arizona State University, Tempe, Arizona 85287

Received August 11, 2006; E-mail: nongjian.tao@asu.edu

Abstract: We studied the effect of anchoring groups on the conductance of single molecules using alkanes terminated with dithiol, diamine, and dicarboxylic-acid groups as a model system. We created a large number of molecular junctions mechanically and analyzed the statistical distributions of the conductance values of the molecular junctions. Multiple sets of conductance values were found in each case. The I - V characteristics, temperature independence, and exponential decay of the conductance with the molecular length all indicate tunneling as the conduction mechanism for these molecules. The prefactor of the exponential decay function, which reflects the contact resistance, is highly sensitive to the anchoring group, and the decay constant is weakly dependent on the anchoring group. These observations are attributed to different electronic couplings between the molecules and the electrodes and alignments of the molecular energy levels relative to the Fermi energy level of the electrodes introduced by different anchoring groups. For diamine and dicarboxylic-acid groups, the conductance values are sensitive to pH due to protonation and deprotonation of the anchoring groups. Further insight into the binding strengths of these anchoring groups to gold electrodes is obtained by statistically analyzing the stretching length of molecular junctions.

Introduction

A basic goal in molecular electronics is to measure and control electron transport through a molecule attached to two electrodes. To reach this goal, one must not only synthesize molecules with desired functions, but also design proper molecule-electrode contacts. This is because the contacts play a critical role in the electron-transport properties of molecules.¹⁻⁵ One way to optimize the molecule-electrode contacts is to select proper anchoring groups at the two ends of a molecule so that they can bind to the electrodes and, in the mean time, provide efficient electronic coupling between the molecule and the electrodes.⁶ To date, the most widely used anchoring group to adsorb on a gold surface is thiol,⁷ although pyridine,⁸ isocyanide,⁹ selenium,¹⁰⁻¹² and amine¹³ have also been studied.

Here we report a systematic study of anchoring-group effect on single-molecule conductance using N -alkanes as a model system.¹⁴⁻¹⁶ N -Alkanes are chosen because they are relatively simple. These molecules are considered to be poorly conducting due to the large HOMO-LUMO gap. By varying N , the number of methylene ($-\text{CH}_2$) groups, one can systematically study the molecular length dependence without significantly changing the HOMO-LUMO gap, which makes it easier to isolate the molecule-electrode contact effects from other factors. We study and compare three anchoring groups, carboxylic acid ($-\text{COOH}$), amine ($-\text{NH}_2$), and thiol ($-\text{SH}$). These anchoring groups bind to gold electrodes via different strengths. For example, $-\text{SH}$ has been known to form strong $\text{S}-\text{Au}$ covalent bonds. $-\text{NH}_2$ -terminated alkanes form stable monolayer on gold nanocrystals, and the binding of amine to gold surface is best described by a weak covalent binding.^{17,18} $-\text{COOH}$ also binds to gold electrodes as evidenced by electrochemical experiments.^{19,20} The binding nature of $-\text{COOH}$ to gold is not yet completely

- (1) Beebe, J. M.; Engelkes, V. B.; Miller, L. L.; Frisbie, C. D. *J. Am. Chem. Soc.* **2002**, *124*, 11268-11269.
- (2) Ke, S. H.; Baranger, H. U.; Yang, W. T. *J. Am. Chem. Soc.* **2004**, *126*, 15897-15904.
- (3) Basch, H.; Cohen, R.; Ratner, M. A. *Nano Lett.* **2005**, *5*, 1668-1675.
- (4) Hu, Y. B.; Zhu, Y.; Gao, H. J.; Guo, H. *Phys. Rev. Lett.* **2005**, *95*, 156803.
- (5) Muller, K. H. *Phys. Rev. B* **2006**, *73*, 045403.
- (6) Xue, Y. Q.; Ratner, M. A. *Phys. Rev. B* **2004**, *69*, 085403.
- (7) Ulman, A. *Chem. Rev.* **1996**, *96*, 1533-1554.
- (8) Xu, B. Q.; Xiao, X. Y.; Tao, N. J. *J. Am. Chem. Soc.* **2003**, *125*, 16164-16165.
- (9) Kim, B.; Beebe, J. M.; Jun, Y.; Zhu, X. Y.; Frisbie, C. D. *J. Am. Chem. Soc.* **2006**, *128*, 4970-4971.
- (10) Patrone, L.; Palacin, S.; Bourgoin, J. P. *Appl. Surf. Sci.* **2003**, *212*, 446-451.
- (11) Patrone, L.; Palacin, S.; Charlier, J.; Armand, F.; Bourgoin, J. P.; Tang, H.; Gauthier, S. *Phys. Rev. Lett.* **2003**, *91*, 096802.
- (12) Yasuda, S.; Yoshida, S.; Sasaki, J.; Okutsu, Y.; Nakamura, T.; Taninaka, A.; Takeuchi, O.; Shigekawa, H. *J. Am. Chem. Soc.* **2006**, *128*, 7746-7747.

- (13) Venkataraman, L.; Klare, J. E.; Tam, I. W.; Nuckolls, C.; Hybertsen, M. S.; Steigerwald, M. L. *Nano Lett.* **2006**, *6*, 458-462.
- (14) Li, X. L.; He, J.; Hihath, J.; Xu, B. Q.; Lindsay, S. M.; Tao, N. J. *J. Am. Chem. Soc.* **2006**, *128*, 2135-2141.
- (15) Wang, W. Y.; Lee, T.; Reed, M. A. *Phys. Rev. B* **2003**, *68*, 035416.
- (16) Wang, W. Y.; Lee, T.; Reed, M. A. *J. Phys. Chem. B* **2004**, *108*, 18398-18407.
- (17) Leff, D. V.; Brandt, L.; Heath, J. R. *Langmuir* **1996**, *12*, 4723-4730.
- (18) Podstawka, E.; Ozaki, Y.; Proniewicz, L. M. *Appl. Spectrosc.* **2005**, *59*, 1516-1526.
- (19) Zhang, Z. J.; Imae, T. *Nano Lett.* **2001**, *1*, 241-243.
- (20) Zhang, Z. J.; Yoshida, N.; Imae, T.; Xue, Q. B.; Bai, M.; Jiang, J. Z.; Liu, Z. F. *J. Colloid Interface Sci.* **2001**, *243*, 382-387.

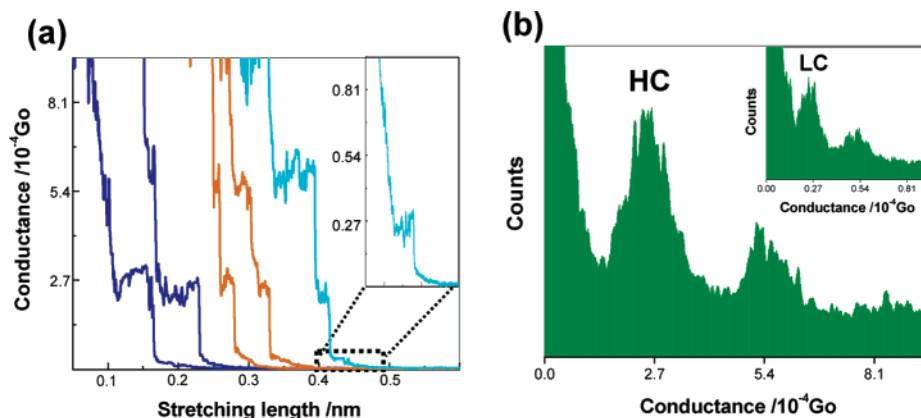


Figure 1. (a) Representative conductance traces recorded during repeated formation and breakdown of dicarboxylic-acid butane molecular junctions. (b) Conductance histograms built by statistically analyzing ~ 450 individual current traces displayed in a. It shows pronounced peaks located at integer multiples of $2.7 \times 10^{-4}G_0$, which corresponds to the conductance of single dicarboxylic-acid butane molecule bound to Au electrodes. This conductance value is denoted as HC. The inset shows a second set of peaks at multiples of $0.27 \times 10^{-4}G_0$, which is marked by LC.

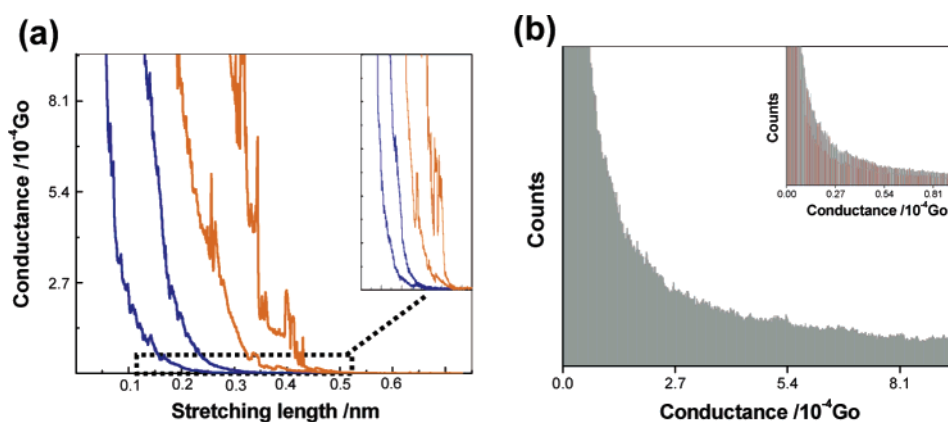


Figure 2. Individual conductance traces of dicarboxylic-acid butane that decay either smoothly (blue) or with oscillating noises (orange). (b) Conductance histograms constructed from the traces as shown in a.

understood, but it is believed that ionic and coordination interactions are at least partially responsible for the binding.²¹

We measure the conductance of *N*-alkanes terminated with these three anchoring groups as a function of molecular length. To determine the conduction mechanism, we also study the temperature dependence of the conductance and current–voltage (*I*–*V*) characteristics of the molecules. To gain further insight into the binding strength of the anchoring groups to the electrodes, we determine the average length over which each electrode–molecule–electrode junction can be mechanically stretched before breakdown. Finally, since the anchoring groups, especially $-\text{NH}_2$ and $-\text{COOH}$, can be protonated or deprotonated by adjusting the solution pH, which may affect their binding strengths to gold electrodes, we perform the experiments in aqueous solutions with different pH.

Experimental Section

We carried out the conductance measurements in a solution containing ~ 1 mM sample molecules using an Au (111) substrate and Au STM tip. The basic procedures are similar to previous works but with some modifications.^{8,14} The first step was to image the substrate in the regular STM mode. Images showing clear and sharp atomic steps are good indications of clean substrate and sharp tip. After surveying the substrate and tip conditions, the tip was parked typically near the center of an atomically flat terrace, and the STM feedback loop was

turned off. At the same time a homemade Labview program was activated to move the tip toward the substrate at a rate of 14–28 nm/s until the current reached a preset value and then retracted. The preset value was chosen to ensure that the tip only gently touched the substrate. During the contacting process, sample molecules may bridge the tip and substrate via the anchoring groups on both ends of a molecule. After reaching the preset value, the tip was pulled back until the current dropped to zero. The above processes were automatically repeated at each bias voltage. To cover a wide current range, we simultaneously recorded the current using two or three scales, differing by 2 or 3 orders of magnitude for each current preamplifier, and repeated the measurements using preamplifiers with different gains.

Since the steps in the individual current traces fluctuate in both current value and length, we collected a large number (~ 1500) of current traces, consecutively without selection, and then performed statistical analysis on the recorded current traces. Typically, the current traces can be divided into three categories: $\sim 30\%$ of the traces show well-defined steps (Figure 1a), $\sim 50\%$ are smooth decay curves (blue curves in Figure 2a) due to direct tunneling between the tip and the substrate, and $\sim 20\%$ are noisy (orange curves in Figure 2a) due to mechanical vibrations of the environment or instability of the molecular junctions. We constructed conductance histograms by projecting each trace onto the vertical axis (current or conductance), so that a long step is shown as a large spike and a short step as a small spike. As a result, long steps carry more weight than short ones. We note that if the step is sloped or noisy, then it results in a peak with a finite width in the projection. Clearly, this counting method avoids the difficulty of distinguishing a noisy feature from a short step and determining the precise position of a step with substantial noise or a slope. Since not

(21) Paik, W. K.; Han, S. B.; Shin, W.; Kim, Y. S. *Langmuir* **2003**, *19*, 4211–4216.

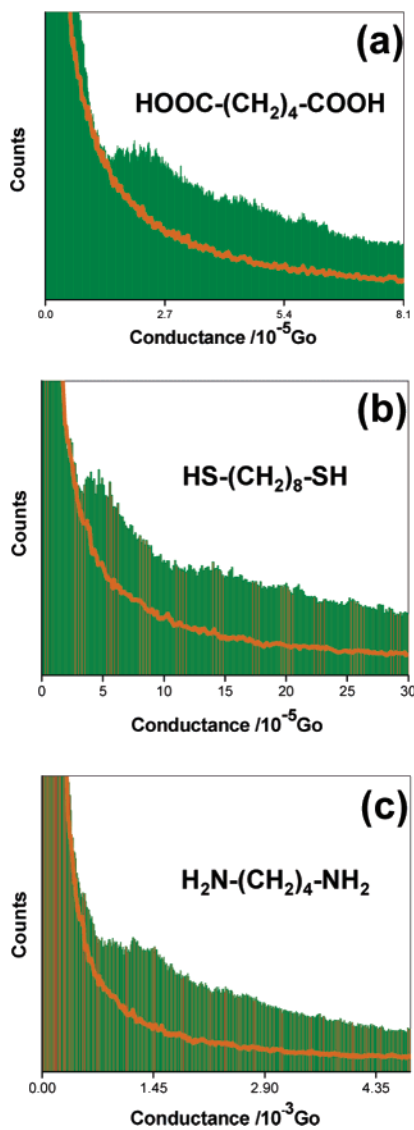


Figure 3. Conductance histograms constructed by including ~ 1500 consecutively current traces without selection (green shaded areas). (a) The histogram of dicarboxylic-acid butane shows a peak located at $2.7 \times 10^{-4} \text{Go}$ (HC). (b) The histogram of octanedithiol shows a peak located at $5.0 \times 10^{-5} \text{Go}$ (LC). (c) The histogram of diamine butane shows a peak at $1.45 \times 10^{-3} \text{Go}$ (HC). The orange lines are the histograms of control experiments performed in the same solutions but containing no sample molecules.

all traces show steps, we constructed conductance histograms using either traces containing steps only or all the traces. In the former case the histogram constructed typically shows two or more well-defined peaks (Figure 1b), and these peaks are broadened in the histogram constructed by including all the traces, but their positions are not affected (green shaded areas in Figure 3).

The Au (111) substrates were prepared by thermally evaporating 130 nm gold on mica in an ultrahigh vacuum chamber. Each substrate was annealed with a H_2 flame and immediately covered with solution. The STM tip was freshly cut from a 0.25 mm gold wire (99.99%) just before each measurement. For experiments carried out in aqueous solutions, the tip was coated with Apiezon wax to minimize ionic leakage current. All chemicals were purchased from commercially available sources (Sigma-Aldrich and Alfa Aesar) and used as received. The alkane molecules terminated with $-\text{COOH}$ and $-\text{NH}_2$ anchoring groups were dissolved in water ($18 \text{ M}\Omega\text{-cm}^{-1}$ from a Nanopure system fed with campus distilled water). The temperature measurements were performed using a Peltier stage with a temperature range from 5 to 65°C .

Results and Discussion

Conductance Measurements. Figure 1b is a representative conductance histogram for dicarboxylic-acid butane constructed from ~ 450 individual conductance traces as shown in Figure 1a. It shows pronounced peaks near $2.7 \times 10^{-4} \text{Go}$ and $2 \times 2.7 \times 10^{-4} \text{Go}$, where $\text{Go} = 2e^2/h \approx 77.4 \mu\text{S}$. According to previous work done by us^{8,14,22} and other groups,^{13,23,24} the peak at $2.7 \times 10^{-4} \text{Go}$ can be assigned to conductance of a single dicarboxylic-acid butane molecule bound to two Au electrodes. We searched conductance peaks between 10^{-6}Go and $\sim 1 \text{Go}$, where the lower limit is the noise level of the current amplifier and the upper limit is the conductance of a single-atom contact between the tip and substrate, and found another set of pronounced peaks located at integer multiples of $0.27 \times 10^{-4} \text{Go}$ (inset of Figure 1b). We refer to the higher conductance value of $2.7 \times 10^{-4} \text{Go}$ as HC and the lower one at $0.27 \times 10^{-4} \text{Go}$ as LC. The HC and LC steps are usually observed in separate traces, but they can also appear in the same trace, e.g., the cyan curve shown in Figure 1a. The overall occurrence of HC is about 3 times greater than that of LC. We observed similar multiple sets of conductance peaks in the histograms of alkanedithiols and attributed them to different contact geometries of the anchoring group to the electrodes.¹⁴ Fujihira et al. also reported multiple sets of peaks in their STM-break junction studies of single-molecule conductance under UHV conditions.²⁵ In the case of alkanedithiols, HC and LC differ by a factor of 4–5, but the conductance difference for dicarboxylic-acid-terminated alkanes is about 10.

As mentioned above, we obtained Figure 1b by analyzing the conductance traces with steps. The peaks in these histograms reflect the preferential occurrence of the steps. In contrast, the histograms constructed from the rest of the traces, i.e., including exponential decay and noisy traces, are completely featureless (Figure 2b). We also constructed conductance histograms by including all of the individual traces (Figure 3). The peaks are broadened due to the increase in the background counts, but they can still be resolved. The first peak position for dicarboxylic-acid butane is located at $2.7 \times 10^{-4} \text{Go}$, almost the same value as that of Figure 1b. The results and conclusions are similar for amine- and thiol-terminated alkanes (Figure 3b and 3c, respectively). Our results appear to be different from a recent report that no conductance peaks can be observed in the histograms of dithiol-terminated alkanes.²⁶ The difference could be due to different experimental procedures rather than intrinsic properties of thiol–gold contacts or methods used for construction of the histograms.

Figure 4a shows a typical conductance histogram for diamine butane constructed from 30% of ~ 1500 individual conductance curves shown in Figure 4b. The histogram displays pronounced peaks located near integer multiples of $1.45 \times 10^{-3} \text{Go}$, significantly higher than that of dicarboxylic-acid butane. This conductance value is in good agreement with that found by

- (22) Xu, B. Q.; Tao, N. J. *J. Science* **2003**, *301*, 1221–1223.
- (23) Hais, W.; van Zalinge, H.; Higgins, S. J.; Bethell, D.; Hobenreich, H.; Schiffrin, D. J.; Nichols, R. J. *J. Am. Chem. Soc.* **2003**, *125*, 15294–15295.
- (24) He, J.; Chen, F.; Li, J.; Sankey, O. F.; Terazono, Y.; Herrero, C.; Gust, D.; Moore, T. A.; Moore, A. L.; Lindsay, S. M. *J. Am. Chem. Soc.* **2005**, *127*, 1384–1385.
- (25) Ishizuka, K.; Suzuki, M.; Fujii, S.; Takayama, Y.; Sato, F.; Fujihira, M. *Jpn. J. Appl. Phys.* **2006**, *45*, 2037–2040.
- (26) Ulrich, J.; Esrail, D.; Pontius, W.; Venkataraman, L.; Millar, D.; Doerr, L. H. *J. Phys. Chem. B* **2006**, *110*, 2462–2466.

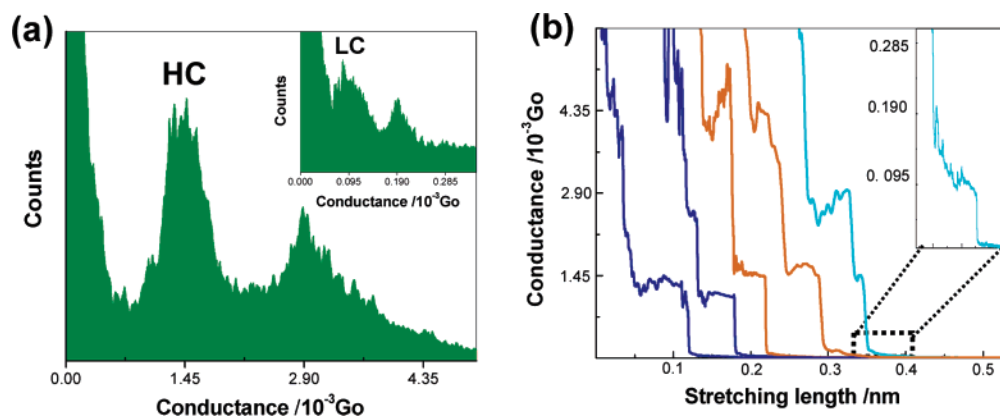


Figure 4. (a) Conductance histograms of diamine butane. The HC and LC peaks are positioned at integer multiples of $1.45 \times 10^{-3}\text{Go}$ and $0.095 \times 10^{-3}\text{Go}$, respectively. (b) Typical conductance traces recorded during formation and breakdown of diamine butane junctions.

Venkataraman et al.¹³ obtained using a different procedure.²⁷ Like dicarboxylic-acid butane and alkanedithiol, diamine butane also shows another set of peaks located at integer multiples of $0.095 \times 10^{-3}\text{Go}$ (inset of Figure 4a), which is ~ 15 times smaller than the value of HC peaks.

Thus far, two sets of peaks have been found in the conductance histograms of alkanes terminated with dithiols, diamines, and dicarboxylic acids, indicating they are probably an inherent feature in the break junction measurements of single molecules. Since the method works by repeatedly creating molecular junctions, the contact geometry between the anchoring groups of the molecules and the gold atoms of the electrodes is expected to vary considerably from one junction to another. This variability is reflected by the finite widths of the peaks in the conductance histograms, and the peak positions give only the conductance of the most probable contact configuration. Thus, it is possible, in principle, that several highly probable contact configurations lead to multiple sets of peaks for a given anchoring group.⁵ This suggestion is supported by the observations (shown below) that both sets of peaks depend on the molecular length, temperature, and pH in similar ways, and they have also similar current–voltage characteristic curves.

Temperature Effect on Conductance. Electron transport along a molecular wire is often described in terms of superexchange and sequential hopping mechanisms. The former is a coherent tunneling process and conductance is temperature independent. In contrast, the latter involves thermal activation and conductance is expected to be sensitive to temperature. Wang et al.¹⁵ measured the conductance of self-assembled alkanethiol monolayer and found that it is independent of temperature over a wide temperature range. Li et al.¹⁴ studied the temperature effect on the single-molecule conductance of alkanedithiols and also observed no significant temperature dependence of the conductance. These studies are consistent with the superexchange mechanism. However, Haiss et al.²⁸ reported temperature dependence of alkanedithiol conductance which was interpreted in terms of thermal fluctuation of the conformations of the molecules.

In order to understand the conduction mechanism of *N*-alkanes terminated with different anchoring groups, we measured the conductance as a function of temperature. Figure 5a

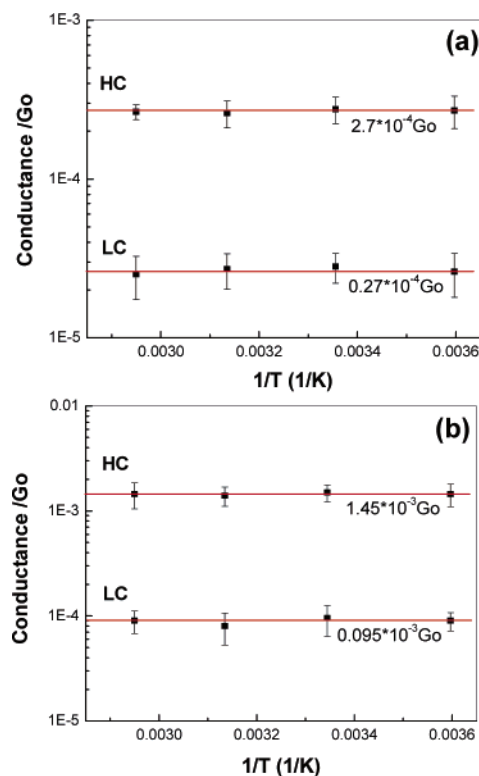


Figure 5. Conductance vs temperature plots for dicarboxylic-acid (a) and diamine (b) butanes. The conductance values are determined by fitting the first peak in each conductance histogram with Gaussian functions, and the error bars are the full widths at half-maximum (fwhm) conductance.

shows the HC and LC values for dicarboxylic-acid butane vs $1/T$; both sets of conductance are independent of temperature within the temperature range of the experimental setup. We note that all the conductance values have been determined by fitting the first peak in each conductance histogram with a Gaussian function, and the error bars are determined by full width at half-maximum (fwhm) conductance, which reflects the distribution of different molecule–electrode contact geometries. The uncertainties of the peak positions as determined by performing Gaussian fitting are much smaller. The conductance values for diamine-terminated alkanes are also independent of temperature (Figure 5b). The temperature independence suggests that superexchange is the dominant conduction mechanism through the alkane chains terminated with dicarboxyl acid, diamine, and dithiol groups.

(27) Venkataraman, L.; Klare, J. E.; Nuckolls, C.; Hybertsen, M. S.; Steigerwald, M. L. *Nature* **2006**, *442*, 904–907.

(28) Haiss, W.; van Zalinge, H.; Bethell, D.; Ulstrup, J.; Schiffrin, D. J.; Nichols, R. J. *Faraday Discuss.* **2006**, *131*, 253–264.

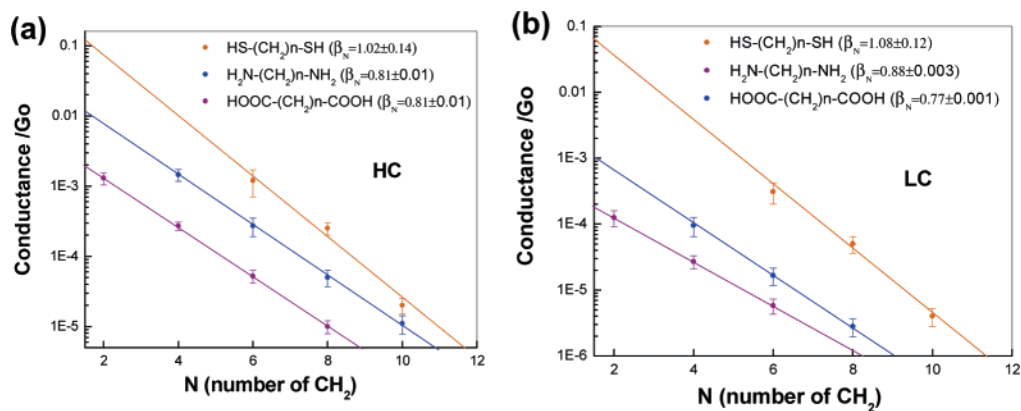


Figure 6. Logarithmic plots of single-molecule conductance vs molecular length for dithiol- (orange), diamine- (blue), and dicarboxylic-acid-terminated (purple) alkanes: (a) HC and (b) LC. Each conductance value is determined by fitting the first peak of the conductance histogram of each molecule with a Gaussian function, and the corresponding error bar is the full width at half-maximum (fwhm) conductance. The solid lines are the linear fits that yield β_N shown in the figures and also in Table 1.

Table 1. β and A for Three Anchoring Groups

	Au-SH-(CH ₂) _n -SH-Au junctions	Au-NH ₂ -(CH ₂) _n -H ₂ N-Au junctions	Au-COOH-(CH ₂) _n -HOOC-Au junctions
HC			
β_N^a	1.02(±0.14)	0.81(±0.01)	0.81(±0.01)
β^a	0.81(±0.11)	0.65(±0.01)	0.61(±0.01)
A_N	0.66(±1.37)Go	0.037(±0.004)Go	0.007(±0.0005)Go
LC			
β_N	1.08(±0.12)	0.88(±0.003)	0.77(±0.001)
β	0.87(±0.08)	0.70(±0.003)	0.57(±0.01)
A_N	0.22(±0.36)Go	0.0032(±0.00006)Go	0.0006(±0.00002)Go

^a β_N and β denote the decay constant per $-\text{CH}_2$ unit and Angstrom, respectively.

Length Dependence of Conductance. In addition to temperature independence, the superexchange mechanism predicts that the conductance decreases exponentially with molecular length, while the hopping mechanism predicts a weaker conductance dependence on molecular length. We thus measured N -alkanes terminated with diamine and dicarboxylic-acid anchoring groups as a function of molecular length by varying the number of $-\text{CH}_2$ units in the alkane chain. The measured conductance values in logarithmic scale together with the value of dithiol-terminated alkanes are plotted in Figure 6. As mentioned above, the error bars are determined from fwhm of the first peak in each conductance histogram. All data sets can be described by $G = A_N \exp(-\beta_N N)$,²⁹ where G is the conductance and N the number of methylene units, which strongly suggests superexchange as the conduction mechanism in all molecules. A_N is a constant determined by the molecule-electrode coupling strength and reflects the contact resistance. β_N is the tunneling decay constant, an important parameter that describes the efficiency of electron transport along the molecules. A_N and β_N , for all the three anchoring groups and for both HC and LC peaks, are listed in Table 1.

A_N is highly sensitive to the type of anchoring group. For example, A_N (HC) varies in the order of 0.66Go, 0.037Go, and 0.007Go for dithiol-, diamine-, and dicarboxylic-acid-terminated alkanes, respectively. For the LC set, A_N (LC) varies in the same order. On the basis of this observation, one may intuitively conclude that the S-Au bond gives the smallest contact resistance while the COOH-Au bond has the highest

contact resistance. It is interesting to consider the binding strengths of these anchoring groups on Au. The best-studied case is Au-S, which has a binding energy of ~ 40 kcal/mol.⁷ However, Au-N and Au-O bond strengths for $-\text{NH}_2$ and $-\text{COOH}$ adsorption on Au are estimated to be the order of 8 and 2 kcal/mol, respectively.³⁰ Thus, the contact resistance appears to correlate with the binding strengths of three contacts: stronger binding gives a lower contact resistance. While it is not clear if the observed correlation is general, the anchoring group of a molecule is expected to affect the electronic coupling between the molecule and the electrode and thus the contact resistance. One factor that the anchoring group might affect the electronic coupling between the molecular core (alkane) and the electrodes is the size of the anchoring group. The distance between the first C atom of alkanethiols and Au (111) (hollow sites) is 3.72 Å according to calculations by Sellers.³¹ We are not aware of any reports on the corresponding distances for amine and carboxylic-acid alkanes, but the distances estimated from the atomic radii are 3.88 and 4.69 Å for amine and carboxylic acid, respectively. Assuming an exponential decay in the electronic coupling with a decay constant of 1 \AA^{-1} , the corresponding ratio in the coupling for carboxylic acid, amine, and thiol is 1:2.3:2.6, which is much smaller than the differences in the measured contact resistance for these three anchoring groups. Thus, size alone does not seem to explain the observation.¹⁰

We also observed differences in β_N between different anchoring groups with a trend $\beta_N(\text{dithiol}) > \beta_N(\text{diamine}) \geq \beta_N(\text{dicarboxylic acid})$. β_N values, ranging between ~ 0.8 and ~ 1.0 per $-\text{CH}_2$ unit or between 0.6 and 0.8 \AA^{-1} , are close to the values reported in the literature.³² The differences in β_N are small for three anchoring groups, but the small difference can significantly affect long-distance electron transport in the molecules due to the exponential dependence of the conductance on length. Both experimental evidence⁹ and theoretical calculations^{33–35} indicate that β_N depends on the alignment of the molecular

(30) Tarazona-Vasquez, F.; Balbuena, P. B. *J. Phys. Chem. B* **2004**, *108*, 15992–16001.

(31) Sellers, H.; Ulman, A.; Shnidman, Y.; Eilers, J. E. *J. Am. Chem. Soc.* **1993**, *115*, 9389–9401.

(32) Wang, W. Y.; Lee, T. H.; Reed, M. A. *Proc. IEEE* **2005**, *93*, 1815–1824.

(33) Yaliraki, S. N.; Kemp, M.; Ratner, M. A. *J. Am. Chem. Soc.* **1999**, *121*, 3428–3434.

(34) Tomfohr, J. K.; Sankey, O. F. *Phys. Rev. B* **2002**, *65*, 245105.

(35) Xue, Y. Q.; Datta, S.; Ratner, M. A. *J. Chem. Phys.* **2001**, *115*, 4292–4299.

(29) Magoga, M.; Joachim, C. *Phys. Rev. B* **1997**, *56*, 4722–4729.

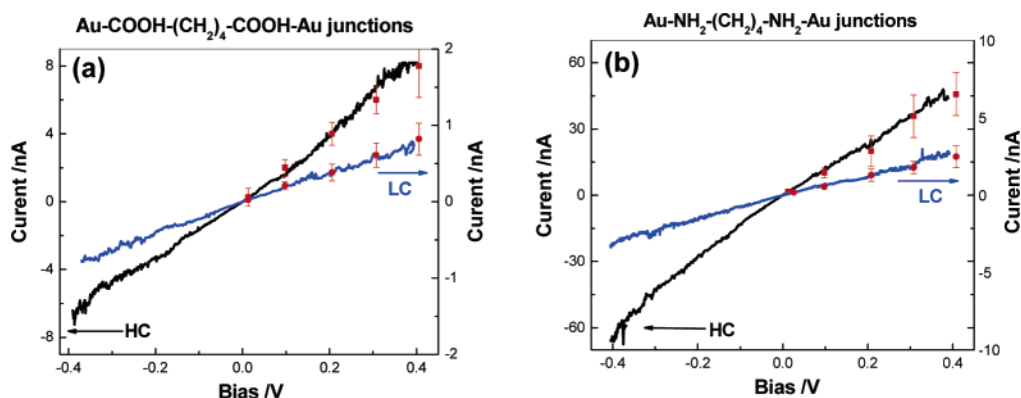


Figure 7. I - V characteristics of HC and LC for dicarboxylic-acid butane (a) and diamine butane (b). The solid circles are determined by measuring the position of the first peak in the current histogram as a function of bias voltage, and the solid curves are recorded by sweeping the bias voltage after formation of individual molecular junctions.

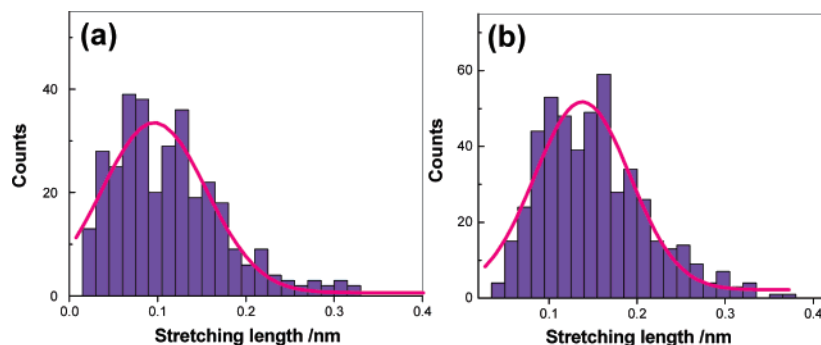


Figure 8. Stretching length histograms for the HC of dicarboxylic-acid (a) and diamine (b) butane. The stretching rate of the STM tip is 14 nm/s, and the bin size is 0.015 nm.

energy levels relative to the Fermi energy level of the electrodes. Recent UPS measurements^{9,11} and calculations⁶ have shown that different anchoring groups can change the energy level alignment. On the basis of these considerations, the observed differences in β_N may be attributed to the differences in the energy alignments.

Current–Voltage Characteristics. Current–voltage (I - V) characteristics can provide important insight into the electron transport through molecules. To measure the I - V curves, we used two approaches: The first is to measure the current histograms at different bias voltages and plot the current extracted from the position of the first peak vs bias (red solid circles in Figure 7). The second is to drive the tip toward the substrate using a voltage supplier to manually control the STM tip position and then pull the tip away from the substrate. When the conductance decreases to a stable current plateau, corresponding to formation of a single molecular junction, we fix the tip position and measure the current while sweeping the bias voltage (the black line for HC and the blue one for LC, respectively). Both methods produce I - V curves that are linear within the applied bias range for all anchoring groups, which are consistent with the tunneling conduction mechanism. We attempted to expand the bias range. In the case of dithiols, the I - V curves are linear for $|V| < 0.5$ V, beyond which they begin to deviate from linear behavior. However, for diamines and dicarboxylic acids, the current became increasingly noisy if the bias was set over +0.4 V or below -0.4 V due to the increased instability of the molecule–electrode contacts at high bias. This smaller stable bias window for diamines and dicarboxylic acids is consistent with their relatively weak binding strengths to gold.

Statistical Analysis of Stretching Length. We discussed that conductance decreases in abrupt steps during the separation stage of the STM tip from a substrate, corresponding to the breakdown of individual molecules from contacting the electrodes. An important parameter closely related to the binding strength is the distance over which the last molecule can be stretched before breakdown. This distance is referred as stretching length here. As shown in Figures 1a and 4b, the stretching length varies from run to run. It is thus necessary to perform statistical analysis on a large number of conductance traces. Figure 8a and b demonstrates the stretching length histograms for the HC of dicarboxylic-acid butane and diamine butane, respectively. To construct these histograms we only count the length of the steps whose conductance value is located in the area that the first conductance peaks cover. The peaks, corresponding to the most probable stretching lengths, are ~ 0.10 and ~ 0.14 nm for the dicarboxylic-acid- and diamine-terminated alkanes, respectively. In the case of octanedithiol, the most probable length is ~ 0.19 nm under the same conditions. We also analyzed the average stretching length for the LC of three molecules, and no visible difference has been observed compared to that of HC. The stretching length data suggests that the S–Au contact is hardest to break and COOH–Au is the easiest to break while NH₂–Au is in between.

pH Dependence. The bindings of carboxylic acid and amine onto Au electrodes are expected to be sensitive to the pH of the solution in which the measurement is carried out. For example, pK_1 and pK_2 for diamine butane are 9.35 and 10.82, respectively. Thus, the amine group is expected to be protonated and exist in the positively charged form (NH₃⁺) in the solution

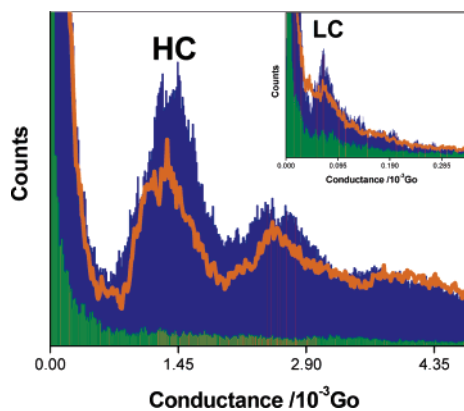


Figure 9. Conductance histograms of diamine butane measured at pH = 1 (green shaded area), 10 (orange line), and 13 (blue shaded area) for HC. The corresponding results for LC are shown in the inset.

with pH below 9. However, if pH is increased above 11, most of the amine groups should be deprotonated and both N atoms are in the form of $-\text{NH}_2$ in which the lone pair electrons can bind strongly to the electrodes. When the pH is between 9 and 11, both acid and base forms are present in solution, but only the deprotonated $-\text{NH}_2$ can interact with Au, so that the conductance value should be close to that in high pH.

Figure 9 compares the conductance histograms of diamine butane in aqueous solutions with pH adjusted at three different pH values. At pH = 13 (in 0.1 M NaOH), the conductance histograms show pronounced peaks with the first peak located near at $1.45 \times 10^{-3}\text{Go}$ (blue shaded area in Figure 9). At this pH the diamine molecules are deprotonated and expected to have a great chance to be trapped between the tip and the substrate electrodes to form molecular junctions. Reducing pH to ~ 10 , the peaks can still be identified in the histogram (the orange curve) but are less pronounced than those at higher pH. The first peak is located at $1.45 \times 10^{-3}\text{Go}$, which is about the same as that for pH 13. When the pH is adjusted to ~ 1 by adding 0.1 M HClO_4 to water, most of the current traces show the smooth exponential decay and the corresponding histogram is essentially featureless (green shaded area in Figure 9). Thus, we conclude that at low pH values no molecular junctions are formed during the stretching. This observation can be understood by the following considerations. At low pH the amine groups are protonated and the N atoms in the amine groups donate their lone pairs of electrons to H ions, which weakens their ability to bind to Au. We observed similar changes on the pH dependency of the LC of the diamine butane (inset of Figure 9), which is consistent with the suggestion that the two sets of conductance peaks are associated with different binding geometries of anchoring groups to the electrodes.

Figure 10 shows the conductance histograms of dicarboxylic-acid butane at three pH values. The $\text{p}K_1$ and $\text{p}K_2$ of dicarboxylic-acid butane are 4.42 and 5.41, respectively. Unlike diamine-terminated alkanes, well-defined peaks are observed in both protonated and deprotonated dicarboxyl acid butane, but the conductance values depend on the pH. At pH = 1, both $-\text{COOH}$ groups are protonated but the O atoms can still interact with Au electrodes via coordination interactions because every O atom possesses two lone pairs of electrons, even though the O atom is more electronegative than Au. The average conductance determined from the HC histogram is $\sim 1.5 \times 10^{-4}\text{Go}$ (green shaded area in Figure 10). At pH = 13, the terminal groups of

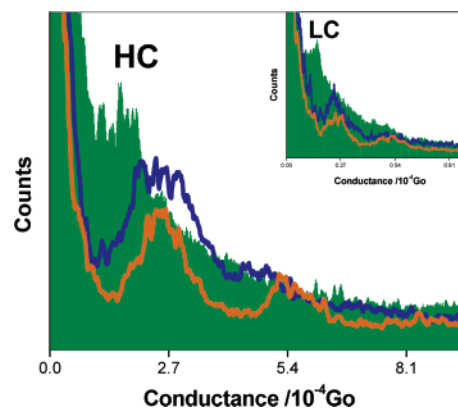


Figure 10. Conductance histograms of dicarboxylic-acid butane measured at pH = 1 (green shaded area), 5 (orange line), and 13 (blue shaded area) for HC. The comparison of LC is shown in the inset.

the molecules are deprotonated to $-\text{COO}^-$ with a negative charge conjugated between the two O atoms, which should enhance the binding ability of the anchoring groups to Au electrodes. The stronger binding has been confirmed by the higher conductance of $2.7 \times 10^{-4}\text{Go}$ (blue curves in Figure 10), which is nearly twice that at pH = 1. When pH is between $\text{p}K_1$ and $\text{p}K_2$, both $-\text{COO}^-$ and $-\text{COOH}$ are present in solution and probably form junctions. For example, the pH is around 5 if we dissolve 1 mM dicarboxylic-acid butane in pure water. In this case, although the peak near $2.7 \times 10^{-4}\text{Go}$ is still visible in the conductance histogram (orange line in Figure 10), it is less pronounced than that at higher pH. For the LC set, we observed a similar pH dependence of the conductance, as shown in the inset of Figure 10.

For both diamine- and dicarboxylic-acid-terminated alkanes pH has a significant effect on either formation of the molecular junction or the conductance value due to protonation/deprotonation of the anchoring groups. In contrast, for dithiol-terminated alkanes, no significant pH dependence of the conductance was observed.³⁶

Conclusions

We systematically studied and compared single-molecule conductance of alkanes terminated with dicarboxylic-acid, diamine, and dithiol anchoring groups. The conductance values of these molecules are independent of temperature (within the temperature range fixed by the setup), indicating coherent tunneling rather than sequential hopping as the conduction mechanism in all alkanes. For each anchoring group conductance decays exponentially with the molecular length, given by $G = A_N \exp(-\beta_N N)$, which also suggests the tunneling mechanism. The prefactor of the exponential function, A_N , a measure of contact resistance, is highly sensitive to the type of the anchoring group, which varies in the order of $\text{Au-S} > \text{Au-NH}_2 > \text{Au-COOH}$. This large dependence is attributed to different electronic coupling efficiencies provided by the different anchoring groups between the alkane and the electrodes. The anchoring groups have a small but measurable effect on the exponential decay constant.

The $I-V$ curves are approximately linear for a small bias range. Increasing the bias range causes instability for diamine-

(36) Xiao, X. Y.; Xu, B. Q.; Tao, N. J. *Angew. Chem., Int. Ed* **2004**, *43*, 6148–6152.

and dicarboxylic-acid-terminated alkanes due to weaker binding strengths of amine and carboxylic acid to gold electrode. We obtained the binding strength information by measuring the average length over which one can stretch each molecular junction until it breaks and found that it varies in the order of $\text{Au-S} > \text{Au-NH}_2 > \text{Au-COOH}$. This observation is consistent with the binding strengths of three anchoring groups to gold. The conductance values of diamine- and dicarboxylic-acid-terminated alkanes are sensitive to pH. At lower pH, $-\text{NH}_3^+$ and $-\text{COOH}$ structures dominate in the solution, while at higher

pH, these two groups are deprotonated to form $-\text{NH}_2$ and $-\text{COO}^-$. The ionic species affect the coupling strength between the molecule and Au electrode and thus the molecule conductance.

Acknowledgment. We thank Dr. Wandlowski for helpful discussions and VW, DOE(DE-FG03-01ER45943), and NSF-(CHE-0243423) for financial support.

JA065864K